Organic LETTERS

Letter

pubs.acs.org/OrgLett

Mechanostereoselective One-Pot Synthesis of Functionalized Head-to-Head Cyclodextrin [3]Rotaxanes and Their Application as Magnetic Resonance Imaging Contrast Agents

Jean Wilfried Fredy,[†,∥] Jérémy Scelle,[†,∥] Gregory Ramniceanu,[‡] Bich-Thuy Doan,[‡] Célia S. Bonnet,[§] Éva Tóth,[§] Mickaël Ménand,[†] Matthieu Sollogoub,[†] Guillaume Vives,*[,†] and Bernold Hasenknopf*[,†]

[†]Sorbonne Universités, UPMC Univ Paris 06, CNRS, Institut Parisien de Chimie Moléculaire UMR 8232, 4 place Jussieu, 75005 Paris, France

[‡]Chimie ParisTech, CNRS, UMR8258 INSERM U1022 Unité de Technologies Chimiques et Biologiques pour la Santé, 11 rue Pierre & Marie Curie, 75005 Paris, France

[§]Centre de Biophysique Moléculaire, CNRS UPR4301, Université d'Orléans, Rue Charles Sadron, 45071 Cedex 2 Orléans, France

Supporting Information

ABSTRACT: A versatile, five-component, one-pot synthesis of cyclodextrin (CD) [3]rotaxanes using copper-catalyzed azide−alkyne cycloaddition has been developed. Head-to-head [3]rotaxanes of α-CD selectively functionalized by one or two gadolinium 1,4,7,10-tetraazacyclododecane-1,4,7-triacetic acid monoamide complexes were obtained mechanostereoselectively. The magnetic resonance imaging efficiency, expressed by the longitudinal proton relaxivity of the rotaxanes, was significantly improved as compared to the functionalized CD. In vitro and in vivo preclinical studies showed a higher contrast and retention in the kidney than gadolinium 1,4,7,10-tetraazacyclododecane-1,4,7,10-tetraacetic acid complex, demonstrating the potential of these rotaxanes as MRI contrast agent.

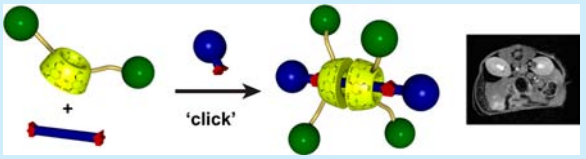

Supramolecular chemistry offers modularity and fast synthesis of complex molecular objects. It is therefore well adapted to biological applications where multifunctional and modular devices are needed. Furthermore, in view of in vivo applications and eventual approval by regulatory agencies, the obtention of a single molecular species is preferable. We are particularly interested in the development of multimodal imaging agents using such a modular supramolecular approach. Our concept consists of preparing monofunctional molecular building units that self-assemble in a modular fashion to produce multifunctional imaging agents. A particularly appealing architecture for this are polyrotaxanes composed of different rings threaded on a common axle.[1] However, efficient threading of functionalized rings must be guaranteed, and different mechano isomers, i.e., diastereomers that differ in the orientation of the mechanically bonded rings,[2] can be obtained using this strategy.

While a large variety of macrocycles such as cucurbituril, crown-ether, bis-paraquat, or calixarene have been reported to produce rotaxanes,[2,3] cyclodextrins (CDs) present the particular advantages of being commercially available, cheap, and easily functionalizable.[4] Moreover, CDs are biocompatible and water-soluble, which enables access to hydrosoluble rotaxanes with potential applications in biology and medicine such as imaging.[1,5] Native CDs have been widely used in rotaxanes or polyrotaxanes[6] since the synthesis of the first CD [2]rotaxane described by Ogino.[7] They are usually obtained by threading followed by an end-capping reaction, with the hydrophobic effect as the driving force for the self-assembly process. This requires forming the pseudorotaxane in water and, after isolation or in situ, performing the stoppering reaction in aqueous solution to prevent dethreading. These limitations have shown that (i) few CD rotaxanes described in the literature contain two CDs and (ii) polyrotaxanes assembled with already functionalized CDs remain less explored and form a mixture of orientational mechanoisomers.[8]

Based on the polyammonium−CD polyrotaxanes described by Wenz,[6a,9] we have developed polyrotaxanes with Gd-functionalized CDs[1] that showed improved relaxivities compared to small molecules. It was also possible to thread bodipy and Gd-functionalized CDs simultaneously onto the polymer strand, proving the viability of the approach to obtain bimodal agents (fluorescence and MRI). However, they were obtained as a statistical mixture of orientational mechanoisomers, and their high toxicity prevented their use in vivo.

In order to lower their toxicity, to test different functionalized CDs, to obtain single isomeric compounds, and to better understand the intrinsic role of the rotaxane architecture on the MRI properties, we decided to investigate smaller [3]rotaxanes as models for the above-mentioned polyrotaxanes. While various synthetic strategies have been developed for multiple threading of other macrocycles,[10] in particular, the "active-metal template strategy",[11] only a few methods yielding [3]rotaxanes of CDs have been described. Anderson showed that reaction of 2,6-

Received: January 16, 2017
Published: February 21, 2017

DOI: 10.1021/acs.orglett.7b00153
Org. Lett. 2017, 19, 1136−1139

dimethylphenol with bis-diazonioazobenzene in the presence of α-CD gave a tail-to tail [3]rotaxane.[12] Takata has recently reported another one-pot strategy to directly obtain head-to-head [3]rotaxanes of α-CD by using isocyanate stoppers.[13] A solid-phase synthesis yielded a head-to-tail [3]rotaxane,[14] and the coupling of two pseudo[2]rotaxanes gave a tail-to-tail [3]rotaxane.[15] Fort prepared polyrotaxanes with lactose-functionalized α-CD.[8c] Inspired by these results and the use of click chemistry for the stoppering reaction of CD-rotaxanes,[8c,10a,16] we aimed at the development of a new general mechanostereoselective synthetic strategy to produce functionalized CD [3]rotaxanes as single isomers. Herein, we report a versatile five-component one-pot synthesis that was applied to α-CD mono or bifunctionalized by Gd(III) complexes (Scheme 1)

Scheme 1. Synthesis of Head-to-Head [3]Rotaxanes

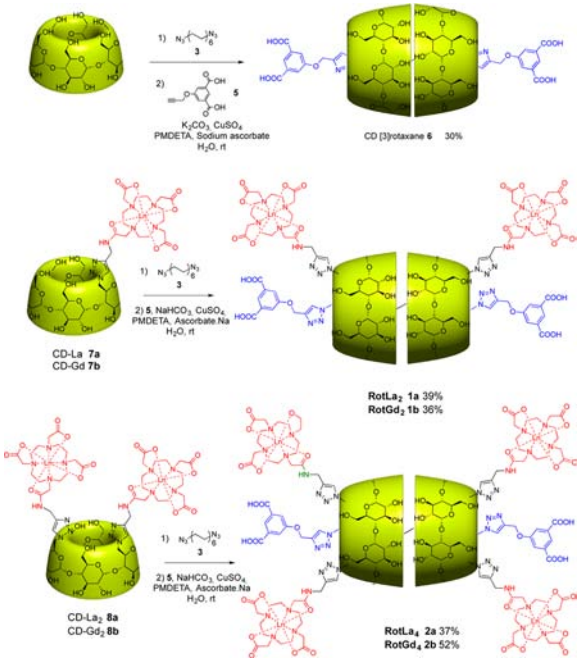

to obtain rotaxane-based MRI contrast agents. In vitro relaxivity of these [3]rotaxanes and their use as biocompatible contrast agents for in vivo imaging in mouse models are also reported.

Rotaxanes were synthesized in a one-pot strategy using a C_{12} alkyl chain as thread and click chemistry for the stoppering reaction. The reaction conditions were optimized using native α-CD (Scheme 1). The diazidododecane axle **3** was, in a first step, mixed with native α-CD in water to yield a pseudorotaxane by the hydrophobic effect. The formation of the inclusion complex can be observed by the appearance of turbidity in the reaction mixture. This is probably due to the formation of tubes of CD pseudorotaxanes and their aggregation via intermolecular hydrogen bonds as observed with other CD polyrotaxanes.[17] In a second step, reactants for copper-catalyzed azide−alkyne cycloaddition (CuAAC) and the stoppers were added to perform the end-capping reaction. The dicarboxylic acid **5** was chosen according to the literature,[16a] as it is described to be large enough to prevent the dethreading of α-CD. Moreover, the carboxylate groups enable the solubility of the rotaxane in water at physiological pH, which is useful for potential in vivo studies.

The ^{1}H DOSY spectrum (diffusion ordered NMR) of the product **6** in DMSO showed the same diffusion coefficient for the protons of the CD, axle, and stoppers (see Figure S1), indicating that they are part of the same supramolecular species. Moreover, the diffusion coefficient is lower than the one of each separate component, which is consistent with the larger molecular size of the assembly. Since DMSO is a solvent that prevents the formation of inclusion compounds with CD,[13] the interlocked structure forms a stable rotaxane. The integration of the ^{1}H NMR spectrum and mass spectrometry (see Figure S5) showed the formation of a single symmetrical [3]rotaxane with two threaded CDs. The 2D T-ROESY spectrum (transverse rotating-frame Overhauser enhancement spectroscopy, Figure 1) provided

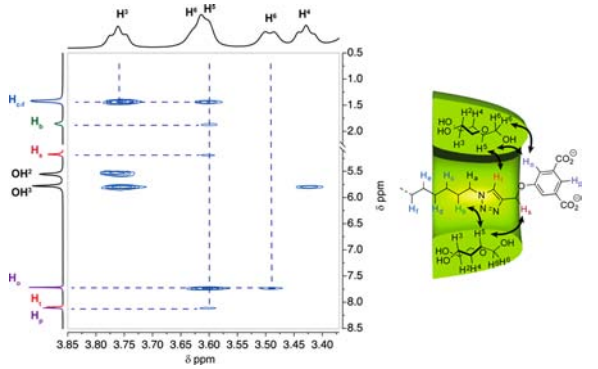

Figure 1. T-ROESY spectrum of [3]rotaxane **6** (600 MHz, DMSO-d_6).

further evidence for the formation of the interlocked structure with correlation peaks between the central axle protons and inner pointing CD protons H^3 and H^5. Moreover, the correlation peak between H^5 and protons H_o, H_t, and H_s as well as H^6 and H_o indicates that the CDs have their primary rim pointing to the stoppers and their secondary rim pointing to each other, hence adopting the head-to-head orientational mechanoisomery. This orientation can be justified by the preferred establishment of hydrogen bonds between the complementary secondary rims[18] and is consistent with other [3]rotaxanes having an alkylene axle.[13]

α-CD was then selectively functionalized by gadolinium complex of 1,4,7,10-tetraazacyclododecane-1,4,7-triacetic acid monoamide (Gd−DO3A-MA) complexes to act as MRI contrast agent. The synthesis is based on a flexible approach using a regioselective deprotection of perbenzylated CDs[19] and a CuAAC[20] between protected mono[21] and bis azido CDs[22] and propargyl-functionalized DO3A-MA followed by deprotection as described in our previous publication.[1] CDs selectively mono- or difunctionalized on diametrically opposed A,D positions on the primary rim by Gd−DO3A-MA complexes were obtained. As MRI is not a very sensitive imaging technique, the difunctionalized CD **8** is particularly interesting in order to increase local Gd(III) concentration.[23] Then, the same procedure was applied for the synthesis of the functionalized CD rotaxanes (Scheme 1), and the products were directly purified by size-exclusion chromatography. The formation of the Gd−CD [3]rotaxanes **$RotGd_2$** and **$RotGd_4$** was confirmed by mass spectrometry (see Figures S6 and S7) with molecular ion peaks at m/z 1292.05 and 1706.14, respectively, corresponding to $[M - 3H]^{3-}$ ions. The rotaxanes were obtained in 35−50% yield, which is suitable for a five-component, one-pot reaction.

Lanthanum analogues (**7a** and **8a**) were also synthesized to obtain further information on the interlocked structure by NMR studies. As observed with native CD, the same diffusion coefficient for the stoppers, functionalized CD and the axle in water were observed in the DOSY spectra for **$RotLa_2$ 1a** and

DOI: 10.1021/acs.orglett.7b00153
Org. Lett. 2017, 19, 1136−1139

RotLa$_4$ 2a (Figurea S2 and S3). For both rotaxanes, correlation peaks between the inner cavity CD H^3 and H^5 and central axle protons on the T-ROESY spectra (Figure S4) confirmed the interlocked structure. Moreover, correlation between H^5 and triazolyl proton H$_t$ indicates that the primary rim of the functionalized CD is pointing to the stoppers. As observed with native CD, this head-to-head configuration enables intramolecular hydrogen bonding between the two secondary rims and seems inherently favored, even though in this case it also avoids the steric hindrance between the substituents on the primary rims.

The effect of the supramolecular assembly on the longitudinal proton relaxivity of the Gd(III) complexes was then investigated by ^{1}H NMRD (nuclear magnetic relaxation dispersion) profiles by measuring T_1 at different magnetic fields. The profiles (Figure 2) were recorded in water at 37 °C for the two rotaxanes (**1b** and

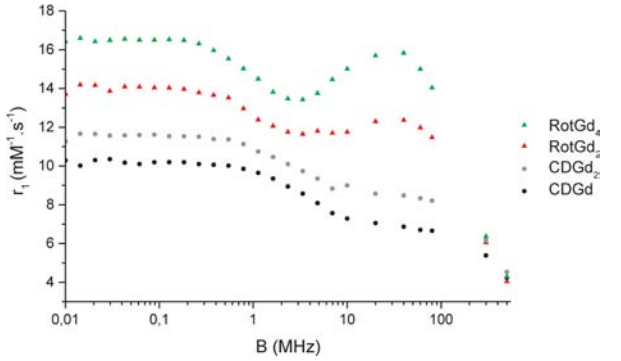

Figure 2. ^{1}H NMRD profiles of aqueous solution of **CD-Gd**, **CD-Gd$_2$**, **RotGd$_2$**, and **RotGd$_4$** at 37 °C.

2b) and compared to the corresponding CDs (**7b** and **8b**). The relaxivities per Gd are considerably higher for **RotGd$_2$ 1b** and **RotGd$_4$ 2b** (12.30 and 15.70 mM^{-1}·s^{-1} at 20 MHz, respectively) than for the parent functionalized CDs (7.06 and 8.57 mM^{-1}·s^{-1}, respectively) or Gd-DOTA[24] (3.83 mM^{-1}·s^{-1}). The relaxivity values are comparable to multimeric Gd−DOTA-functionalized CD systems of similar size ([Gd−DOTA]$_7$-β-CD: 12.2 mM^{-1}·s^{-1} at 60 MHz;[25] Gd−DO3A-HP-β-CD: 7.82 mM^{-1}·s^{-1} at 60 MHz;[5] [Gd−DO3P]$_{6.9}$-F$_{0.1}$-β-CD: 21.6 mM^{-1}·s^{-1} at 20 MHz[26]). The NMRD profile shows an enhancement at medium field (20−80 MHz) for the rotaxanes, which is not present for the functionalized CDs. This hump is characteristic of macromolecular contrast agents (such as polymers or liposomes), and it indicates that the interlocked architecture plays a crucial role in the rotational dynamics and subsequently in the relaxivity properties. The temperature dependence (Table S1) showing an increased relaxivity with increasing temperature is also an indication of the rigidity of the system. Indeed, it proves that the relaxivity is limited by the water-exchange rate of the complex and not by its rotation. It is most notable that our small rotaxanes feature also those properties which were previously observed with polyrotaxanes (CD−Gd/polyammonium PR: 16.4 mM^{-1}·s^{-1};[1] CD−Gd$_2$/polyammonium PR: 19.6 mM^{-1}·s^{-1};[1] Gd−DO3A-HPCD/Pluronic PR: 22.8 mM^{-1}·s^{-1} [5] at 60 MHz). The [3]rotaxanes behave indeed as a typical macromolecular contrast agent with promising relaxation properties at relevant body temperature.

The biodistribution of rotaxanes **RotGd$_2$** and **RotGd$_4$** was then studied in vivo on BALB/c mice using adapted dynamic MRI sequences at 7T. Several regions of interest were monitored (liver and kidney), and the MRI intensities of the regions were plotted pre- and post-injection of the contrast agent at Gd concentration of 50 μmol·kg^{-1}. Comparison with commercial Gd−DOTA as a reference was performed at the same concentration of Gd. Figure 3 shows MRI cross sections where

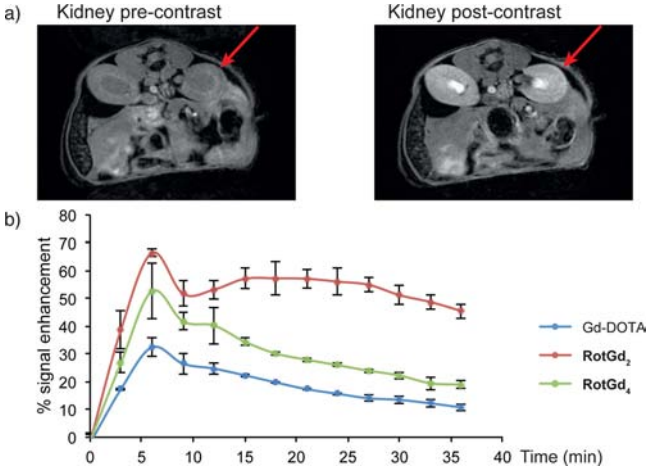

Figure 3. (a) MRI cross sections of the kidneys (red arrow) pre- (left) and postinjection (right, 40 min) of RotGd$_2$. (b) Dynamic MRI signal enhancement in renal cortex after CA injection.

the kidney regions are highlighted as expected for the biodistribution of a molecular scaffold of a small size inferior to 5 nm.[27] Comparison of the pre- and postcontrast images clearly reveals the higher brightness of the kidney caused by **RotGd$_2$**. For further images of the liver with this CA and of kidney and liver with **RotGd$_4$**, see Figures S9 and S10. The peaks of enhancement compared to the precontrast image were observed at the same time, 6 min post-injection for all CA in the liver and the kidney followed by a phase of decay (Figure 3b and Figure S11). The absolute values at 21 min post-injection are highest for **RotGd$_2$** (16% in the liver, 67% in the cortical region of the kidney), followed by those of **RotGd$_4$** (9% and 28% respectively) and Gd−DOTA (6% and 17%, respectively). After bloodstream circulation with a complementary transitory visualization through the vascular network in the liver, the CAs are excreted from the kidney cortex to the bladder. After 40 min, the levels of **RotGd$_4$** and Gd−DOTA came back to their precontrast values and to 10% signal enhancement for **RotGd$_2$** in the liver, indicating a hepatic wash out. However, a stronger retention in the cortical region of the kidney was observed with enhancement of 46% and 19% for **RotGd$_2$** and **RotGd$_4$**, respectively (11% for Gd−DOTA). Both rotaxanes behave similarly in the kidney glomerular and tubular clearance with slower elimination than the mononuclear complex Gd−DOTA. Due to the higher concentration of **RotGd$_2$** than that of **RotGd$_4$** both injected for an identical final Gd amount, **RotGd$_2$** takes longer to be eliminated. This imaging study evidenced that both rotaxanes display higher contrast enhancement than the commercial CA Gd−DOTA over the full observation period without the typical liver accumulation observed for macromolecular agents. Thus, they improve the imaging properties without undesired liver uptake. The relatively long circulation time opens the perspective for vectorization toward other tissues than the kidney.

In summary, we have successfully developed a one-pot, five-component mechanostereoselective synthesis of head-to-head CD [3]rotaxanes leading to the first [3]rotaxanes with Gd−

DOI: 10.1021/acs.orglett.7b00153
Org. Lett. 2017, 19, 1136−1139

DO3A-MA functionalized CDs. These rotaxanes have shown their ability to significantly improve the relaxivity properties compared to parent CDs, indicating the interest of this supramolecular approach for MRI applications. Indeed, the behavior of [3]rotaxanes is already comparable with those of much larger macromolecular agents while keeping the advantages of small molecules in terms of synthesis and characterization at the molecular level. These rotaxanes are nontoxic, and their biodistribution could be investigated by MR imaging with high temporal resolution. Both rotaxanes exhibit higher contrast enhancement and retention than the commercial Gd−DOTA, with a particular improvement for **RotGd$_2$**. In conclusion, rotaxanation is a viable approach to obtain contrast agents with improved efficiency, even when the rotaxanes are relatively small. This simple supramolecular approach has multiple advantages over conventional covalent strategies such as modularity and versatility. Indeed, each component is synthesized and characterized separately before the assembly, and can be exchanged at will by other components.

■ ASSOCIATED CONTENT

Supporting Information

The Supporting Information is available free of charge on the ACS Publications website at DOI: 10.1021/acs.orglett.7b00153.

Experimental procedures, compound characterization data, and NMR spectra (PDF)

■ AUTHOR INFORMATION

Corresponding Authors

*E-mail: guillaume.vives@upmc.fr.
*E-mail: bernold.hasenknopf@upmc.fr.

ORCID

Bernold Hasenknopf: 0000-0002-2518-1405

Author Contributions

‖J.W.F. and J.S. contributed equally.

Notes

The authors declare no competing financial interest.

■ ACKNOWLEDGMENTS

We thank Agnès Pallier, Université d'Orléans, for performing ICP measurements on the Gd^{3+}-containing samples. Financial support from UPMC (programme Emergence) and the LabEx MiChem programme under reference ANR-11-IDEX-0004-02 and from the Ligue contre le Cancer are acknowledged. We thank also the Institut Weizmann Français for the postdoctoral fellowship to G.R. and the IDEX Programme interdisciplinaire, Université Paris Descartes SINON and Université Paris Descartes. for the MRI equipment.

■ REFERENCES

(1) Fredy, J. W.; Scelle, J.; Guenet, A.; Morel, E.; Adam de Beaumais, S.; Ménand, M.; Marvaud, V.; Bonnet, C. S.; Tóth, E.; Sollogoub, M.; Vives, G.; Hasenknopf, B. *Chem. - Eur. J.* **2014**, *20*, 10915.

(2) Neal, E. A.; Goldup, S. M. *Chem. Commun.* **2014**, *50*, 5128.

(3) (a) Sauvage, J.-P.; Dietrich-Buchecker, C. *Molecular Catenanes, Rotaxanes and Knots*; Wiley-VCH, 1999. (b) Amabilino, D. B.; Perez-Garcia, L. *Chem. Soc. Rev.* **2009**, *38*, 1562. (c) Forgan, R. S.; Sauvage, J.-P.; Stoddart, J. F. *Chem. Rev.* **2011**, *111*, 5434. (d) van Dongen, S. F. M.; Cantekin, S.; Elemans, J. A. A. W.; Rowan, A. E.; Nolte, R. J. M. *Chem. Soc. Rev.* **2014**, *43*, 99.

(4) (a) Khan, A. R.; Forgo, P.; Stine, K. J.; D'Souza, V. T. *Chem. Rev.* **1998**, *98*, 1977. (b) Sollogoub, M. *Synlett* **2013**, *24*, 2629. (c) Sollogoub, M. *Eur. J. Org. Chem.* **2009**, *2009*, 1295. (d) Wang, B.; Zaborova, E.; Guieu, S.; Petrillo, M.; Guitet, M.; Blériot, Y.; Ménand, M.; Zhang, Y.; Sollogoub, M. *Nat. Commun.* **2014**, *5*, 5354.

(5) Zhou, Z.; Mondjinou, Y.; Hyun, S.-H.; Kulkarni, A.; Lu, Z.-R.; Thompson, D. H. *ACS Appl. Mater. Interfaces* **2015**, *7*, 22272.

(6) (a) Wenz, G.; Han, B.-H.; Müller, A. *Chem. Rev.* **2006**, *106*, 782. (b) Harada, A.; Hashidzume, A.; Yamaguchi, H.; Takashima, Y. *Chem. Rev.* **2009**, *109*, 5974.

(7) Ogino, H. *J. Am. Chem. Soc.* **1981**, *103*, 1303.

(8) (a) Wang, Z.-B.; Takashima, Y.; Yamaguchi, H.; Harada, A. *Org. Lett.* **2011**, *13*, 4356. (b) Wenz, G.; Von der Bey, E.; Schmidt, L. *Angew. Chem., Int. Ed. Engl.* **1992**, *31*, 783. (c) Chwalek, M.; Auzely, R.; Fort, S. *Org. Biomol. Chem.* **2009**, *7*, 1680. (d) Mondjinou, Y. A.; Hyun, S. H.; Xiong, M.; Collins, C. J.; Thong, P. L.; Thompson, D. H. *ACS Appl. Mater. Interfaces* **2015**, *7*, 23831.

(9) Wenz, G.; Keller, B. *Angew. Chem., Int. Ed. Engl.* **1992**, *31*, 197.

(10) (a) Hänni, K. D.; Leigh, D. A. *Chem. Soc. Rev.* **2010**, *39*, 1240. (b) Beves, J. E.; Blight, B. A.; Campbell, C. J.; Leigh, D. A.; McBurney, R. T. *Angew. Chem., Int. Ed.* **2011**, *50*, 9260. (c) Xue, M.; Yang, Y.; Chi, X.; Yan, X.; Huang, F. *Chem. Rev.* **2015**, *115*, 7398.

(11) (a) Crowley, J. D.; Goldup, S. M.; Lee, A.-L.; Leigh, D. A.; McBurney, R. T. *Chem. Soc. Rev.* **2009**, *38*, 1530. (b) Movsisyan, L. D.; Franz, M.; Hampel, F.; Thompson, A. L.; Tykwinski, R. R.; Anderson, H. L. *J. Am. Chem. Soc.* **2016**, *138*, 1366.

(12) Craig, M. R.; Claridge, T. D. W.; Hutchings, M. G.; Anderson, H. L. *Chem. Commun.* **1999**, 1537.

(13) (a) Akae, Y.; Okamura, H.; Koyama, Y.; Arai, T.; Takata, T. *Org. Lett.* **2012**, *14*, 2226. (b) Akae, Y.; Koyama, Y.; Kuwata, S.; Takata, T. *Chem. - Eur. J.* **2014**, *20*, 17132. (c) Akae, Y.; Koyama, Y.; Sogawa, H.; Hayashi, Y.; Kawauchi, S.; Kuwata, S.; Takata, T. *Chem. - Eur. J.* **2016**, *22*, 5335.

(14) Daniell, H. W.; Klotz, E. J. F.; Odell, B.; Claridge, T. D. W.; Anderson, H. L. *Angew. Chem., Int. Ed.* **2007**, *46*, 6845.

(15) Qu, D. H.; Wang, Q. C.; Ma, X.; Tian, H. *Chem. - Eur. J.* **2005**, *11*, 5929.

(16) (a) Zhao, Y.-L.; Dichtel, W. R.; Trabolsi, A.; Saha, S.; Aprahamian, I.; Stoddart, J. F. *J. Am. Chem. Soc.* **2008**, *130*, 11294. (b) Loethen, S.; Ooya, T.; Choi, H. S.; Yui, N.; Thompson, D. H. *Biomacromolecules* **2006**, *7*, 2501. (c) Ooya, T.; Inoue, D.; Choi, H. S.; Kobayashi, Y.; Loethen, S.; Thompson, D. H.; Ko, Y. H.; Kim, K.; Yui, N. *Org. Lett.* **2006**, *8*, 3159.

(17) Harata, K. *Chem. Rev.* **1998**, *98*, 1803.

(18) Kamitori, S.; Matsuzaka, O.; Kondo, S.; Muraoka, S.; Okuyama, K.; Noguchi, K.; Okada, M.; Harada, A. *Macromolecules* **2000**, *33*, 1500.

(19) Lecourt, T.; Herault, A.; Pearce, A. J.; Sollogoub, M.; Sinaÿ, P. *Chem. - Eur. J.* **2004**, *10*, 2960.

(20) (a) Tornøe, C. W.; Christensen, C.; Meldal, M. *J. Org. Chem.* **2002**, *67*, 3057. (b) Rostovtsev, V. V.; Green, L. G.; Fokin, V. V.; Sharpless, K. B. *Angew. Chem., Int. Ed.* **2002**, *41*, 2596.

(21) Guieu, S.; Sollogoub, M. *Angew. Chem., Int. Ed.* **2008**, *47*, 7060.

(22) (a) Deunf, E.; Zaborova, E.; Guieu, S.; Blériot, Y.; Verpeaux, J.-N.; Buriez, O.; Sollogoub, M.; Amatore, C. *Eur. J. Inorg. Chem.* **2010**, *2010*, 4720. (b) Ménand, M.; Adam de Beaumais, S.; Chamoreau, L.-M.; Derat, E.; Blanchard, S.; Zhang, Y.; Bouteiller, L.; Sollogoub, M. *Angew. Chem., Int. Ed.* **2014**, *53*, 7238.

(23) *The Chemistry of Contrast Agents in Medical Magnetic Resonance Imaging*, 2nd ed.; Merbach, A., Helm, L., Toth, E., Eds.; John Wiley & Sons, 2013.

(24) Powell, D. H.; Dhubhghaill, O. M. N.; Pubanz, D.; Helm, L.; Lebedev, Y. S.; Schlaepfer, W.; Merbach, A. E. *J. Am. Chem. Soc.* **1996**, *118*, 9333.

(25) Song, Y.; Kohlmeir, E. K.; Meade, T. J. *J. Am. Chem. Soc.* **2008**, *130*, 6662.

(26) Kotková, Z.; Kotek, J.; Jirák, D.; Jendelová, P.; Herynek, V.; Berková, Z.; Hermann, P.; Lukeš, I. *Chem. - Eur. J.* **2010**, *16*, 10094.

(27) Soo Choi, H. S.; Liu, W.; Misra, P.; Tanaka, E.; Zimmer, J. P.; Itty Ipe, B.; Bawendi, M. G.; Frangioni, J. V. *Nat. Biotechnol.* **2007**, *25*, 1165.

DOI: 10.1021/acs.orglett.7b00153
Org. Lett. 2017, 19, 1136−1139